Isolation of an ion channel gene from *Arabidopsis thaliana* using the H5 signature sequence from voltage-dependent K^+ channels

Karen A. Ketchum*, Carolyn W. Slayman

Department of Genetics, Yale University School of Medicine, 333 Cedar Street, New Haven, CT 06510, USA

Received 30 October 1995

Abstract **A degenerate oligonucleotide corresponding to the K^+ channel signature sequence (TMTTVGYGD) was used to isolate the genomic and cDNA forms of a new channel gene, *AKT3*, from *Arabidopsis thaliana*. The deduced protein sequence has a predicted membrane topography similar to *Shaker*-like K^+ channels. Three distinct modules comprise the carboxyl-terminal half: a nucleotide-binding motif, an ankyrin repeat domain, and a polyglutamate track. *Xenopus* oocytes injected with cRNA exhibited an inward-rectifying K^+ current, demonstrating that the AKT3 polypeptide is a functional transport protein. Two other *Arabidopsis* K^+ transporters (AKT1 and KAT1) share 60% homology with AKT3; together these proteins constitute a family of plant inward-rectifying K^+ channels.**

Key words: K^+ channel; Inward-rectifier; Plant; *Arabidopsis*; cDNA clone; *Xenopus* oocyte expression

1. Introduction

Potassium ion channels are essential transport proteins in the plasma membrane of plant cells, mediating the flux of K^+ in diverse physiological settings [1,2]. One well studied example is provided by the K^+ channels that are activated during turgor-induced changes in cell shape. The vectorial transport of K^+, accompanied by anion flux, causes large shifts in cytoplasmic osmolarity and ultimately water movement. The resulting alterations in cell size allow guard cells to regulate gas exchange during photosynthesis [3], and underlie leaf movements associated with circadian rhythms, solar tracking, and the thigmonastic response of insectivorous plants [4]. K^+ channels also serve a nutritive function by mediating K^+ entry in high potassium environments, and have been identified with the low-affinity K^+ uptake pathway initially described by Epstein and coworkers [5]. Finally, K^+ channels help maintain membrane potential in circumstances where the plasmalemma conductance exceeds the pumping capacity of the proton ATPase. Situations of this sort are numerous and include routine transport events such as the uptake of sugars and amino acids [6,7], or specialized phenomena like the cellular stress response(s) evoked by severe growth environments [8] or pathogenic attack [9].

It seems likely that several types of K^+ channel must coexist to accommodate these diverse functions. Indeed, electrophysiological recordings of plant protoplasts have identified a variety of voltage-dependent K^+ channels (inward- and outward-rectifiers), as well as voltage-dependent, nonselective cation channels that permit K^+ flux [1,2]. In some species, multiple forms are present. For example, corn suspension cells possess both voltage-dependent and Ca^{2+}- and voltage-dependent K^+ channels that contribute to the outward-rectifying K^+ current observed during whole-cell recording [10]. Similarly, in wheat root protoplasts, there are two kinetically distinct inward-rectifying K^+ currents, both activated by membrane hyperpolarization [11]. In other situations K^+ channel activity is modulated by changes in secondary factors such as cytosolic Ca^{2+} [12,13], intracellular and extracellular pH [14], or trimeric G-proteins [15].

In order to understand at the molecular level how different K^+ channels contribute to the various physiological responses observed in plant cells, it is necessary to begin by determining the primary structure of the channel proteins. Data from both electrophysiological and pharmacological experiments have suggested that plant K^+ channels share structural features with voltage-dependent K^+ channels characterized in animals [1]. Thus, the cloning strategy we employed was to design degenerate oligonucleotides to conserved regions of known K^+ channel genes and then use these probes to identify similar sequences from plant genomic DNA.

Starting with a nucleotide probe corresponding to the highly conserved sequence TMTTVGYGD from the H5 region (or P-region) of voltage-dependent K^+ channels [16] we have cloned the genomic and cDNA forms of a new ion channel gene, *AKT3*, from *Arabidopsis thaliana*. The AKT3 protein has a predicted membrane topography similar to *Shaker*-like K^+ channels with a long carboxyl-terminal extension that contains a nucleotide-binding domain, four ankyrin repeats and a polyglutamate track. Sequence alignments reveal that *AKT3* belongs to a multigene family of inward-rectifying K^+ channels that includes the *Arabidopsis KAT1* and *AKT1* genes, previously isolated by genetic complementation of K^+ transport mutants in yeast [17,18]. However, the percentage of amino acid identity among these three proteins is quite low, suggesting that each channel has a distinct physiological role in plasma membrane K^+ transport.

2. Materials and methods

2.1. Library screening

An *Arabidopsis thaliana* genomic library was screened with a degenerate oligonucleotide made to the conserved K^+ channel sequence, TMTTVGYGD. The oligonucleotide corresponded to the noncoding strand with a 5′ to 3′ sequence of TCI CC(A/G) TAI CC(A/C/G) AC(N) GT(N) GTC AT(N) GT where I, is deoxyinosine and N denotes all four biological deoxynucleotides. The Lambda Dash II library (Stratagene Cloning Systems, La Jolla, CA; generously supplied by Dr. A. Cheung, Department of Biology, Yale University), with an average insert size of 15 kb, was plated by standard methods and 3.8×10^5 plaque forming units, five times the *Arabidopsis* genome, were screened in the initial round. Preparation of nitrocellulose filters and synthesis of the ^{32}P-end-labelled oligonucleotide probe were performed as described in Sam-

*Corresponding author. Fax: (1) (203) 785 7227.

SSDI 0014-5793(95)01417-9

brook et al. [19]. Filters were hybridized at 40°C for 16 hours and then washed at room temperature in 2× SSPE, 0.1% SDS for a total of 30 minutes. Positive plaques were picked and rescreened until each isolate was purified.

2.2. Cloning of the genomic sequence and isolation of the corresponding cDNA

Plate lysates of each library isolate were prepared and bacteriophage particles were purified by differential centrifugation. DNA was subsequently liberated by extraction with phenol. We used the 'alternative methods for purification of bacteriophage λ' [19] without the addition of SDS and with a final precipitation of the phage DNA by sodium acetate (0.2 M) and ethanol.

Genomic DNA inserts were analyzed by Southern blots to identify the TMTTVGYGD binding region. End-labelled oligonucleotide probes and hybridization conditions were the same as described for library screening. The TMTTVGYGD binding region was subcloned into pBluescript (Stratagene Cloning Systems) and sequenced on both strands (Sequenase DNA Sequencing Kit, United States Biochemical, Cleveland, OH). Overlapping clones were later isolated, extending the genomic sequence to the 5′ *Xba*I site and the 3′ *Sst*I site.

cDNA clones were isolated by the polymerase chain reaction (PCR, [19]) from a pooled plasmid sample of an *Arabidopsis* leaf cDNA library (kindly provided by Dr. R. Meagher, Department of Genetics, University of Georgia). Four separate amplification products (amplicons) were obtained which spanned the following regions: exons 1 to 2 (nucleotides 1 to 460, numbers correspond to the genomic sequence shown in Fig. 2), exons 2 through 7 (nucleotides 405 to 2252), exons 5 to 9 (nucleotides 1214 to 2716), and exons 7 through 10 (nucleotides 2048 to 3400). Primers for the N- and C-terminal fragments contained additional nucleotides to generate restriction sites, *Pst*I–*Sac*I prior to the N-terminus and *Spe*I–*Msc*I following the C-terminus, for subsequent cloning into expression vectors. Each amplicon was sequenced on both strands and then the four fragments were assembled at the *Hin*cII (exon 2), *Bgl*II (exon 5), and *Xba*I (exon 8) sites. The complete cDNA was resequenced to confirm that mutations had not been created during the ligation procedure. One nucleotide difference exists between the genomic sequence and cDNA clone used for expression studies, position 2758, where an A to T substitution is present at the wobble position for proline 620. Additional PCR reactions determined that the A→T change developed during DNA amplification and was not due to a genetic polymorphism.

The transcriptional start site was identified by a 5′ RACE (Gibco-BRL, Gaithersburg, MD) from total *Arabidopsis* RNA, isolated with TRIzol (Gibco-BRL), using gene-specific primers complementary to nucleotides 444–460 (5′ CAA GAC AAT GTC AAC CG 3′, GSP1) and 120 145 (5′ CTG GTT ATA GCT AGC AAC ACC AAG TG 3′, GSP2). The polyadenylation site was located in a final amplicon that was obtained by running a PCR reaction from the 19mer starting at nucleotide 3295 in exon 10 (5′ AAG TGA GAC GAT GGT GAC G 3′) to a second primer (5′ TCA CTA TAG GGC GAA TTG GG 3′) situated within the polycloning site of the library vector (pcDNA II, Invitrogen corporation, San Diego, CA).

General molecular biology reagents were obtained from New England Biolabs, Inc. (Beverly, MA) and Boehringer Mannheim Corporation (Indianapolis, IN). Nitrocellulose and nylon filters for library screening and Southern blots were purchased from Schleicher & Schuell (Keene, NH). PCR reagents, Amplitaq and Taq polymerase were purchased from Perkin Elmer (Norwalk, CT). Amplification products were initially cloned with the TA Cloning Kit (Invitrogen Corporation). Analyses of DNA and protein sequences were performed with the GCG software package (Genetics Computer Group, Inc. Madison, WI) available through the Yale Biomedical Computing Unit. Calculation of percent sequence identity was done with the GAP program using a value of zero for both the gap creation penalty and the gap extension penalty.

2.3. Oocyte expression

The complete *AKT3* cDNA was excised at the *Sac*I and *Spe*I restriction sites and subcloned into pGEM-A, which has a polyadenylate track downstream of the multiple cloning site [20]. This construct was subsequently linearized at a *Not*I site 3′ of the poly(A) sequence, and cRNA was synthesized from the T7 promoter using the mMessage mMachine transcription kit (Ambion Inc., Austin, TX). Standard methods for oocyte isolation (*Xenopus laevis*) and cRNA injection were used (recently reviewed by Goldin [21]). Typically, 50 ng of cRNA were injected per oocyte and recordings were made 3–8 days after injection. Two-microelectrode voltage-clamp recordings were obtained with the OC-725 voltage-clamp (Warner Instrument Co., New Haven, CT). Data were acquired with the Pulse software program (HEKA elektronik GmbH, Lambrecht, Germany), and analyses and figure preparation were done using Igor Pro (WaveMetrics, Inc., Lake Oswego, OR).

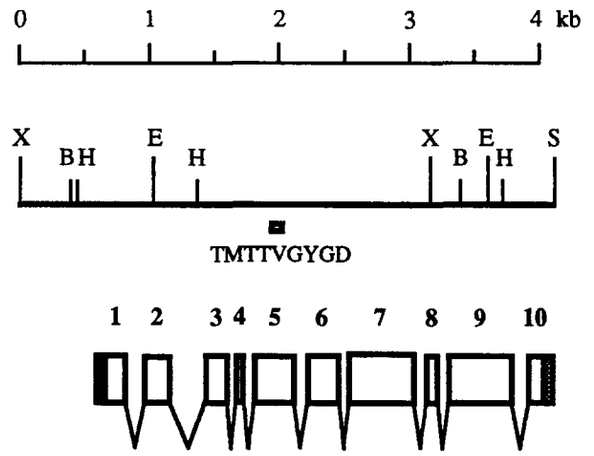

Fig. 1. Restriction enzyme map of the *AKT3* genomic clone and location of exons in the mature message. Abbreviations for restrictions enzymes are as follows: B, *Bam*HI; E, *Eco*RI; H, *Hin*dIII; S, *Sst*I; X, *Xba*I. The full-length cDNA has ten exons (open boxes) with short untranslated regions at both the N- and C-terminus (filled boxes). The oligonucleotide probe, corresponding to the TMTTVGYGD peptide sequence, hybridized with the 2.7 kb *Eco*RI fragment and mapped to exon 5.

3. Results and discussion

Forty-eight positive plaques were selected from the initial library screen. When these isolates were purified and inserts compared by restriction enzyme digests and Southern hybridization to the TMTTVGYGD oligonucleotide, thirteen displayed a common 2.7 kb *Eco*RI fragment that bound the K^+ channel probe. One isolate from this group, PCAT14, was selected for further subcloning and sequencing of the channel gene, which has been designated *AKT3*.

3.1. Genomic organization of the AKT3 gene

The *AKT3* gene is contained within a 4.1 kb fragment delineated by *Xba*I and *Sst*I sites at the 5′ and 3′ ends, respectively (Fig. 1). Ten exons contribute to the mature message which begins at cytosine, position +1 (Fig. 2), and extends for 2.4 kb. The poly(A) tail is appended to nucleotide 3419. Several interesting regulatory elements are present in the 5′ untranslated region. Thirty-three nucleotides prior to the transcriptional start site is a putative TATA box for the binding of transcription factor TFIID. Further upstream at −197 to −201 is the enhancer sequence CCAAT. Along with these common eukaryotic promoter motifs are two additional 5′ elements that may contribute to *AKT3* gene expression. The first is the tetramer ACGT, −157 to −160, which constitutes the core sequence recognized by several plant basic/leucine zipper (bZIP) DNA-binding proteins; *trans*-acting factors in this group frequently

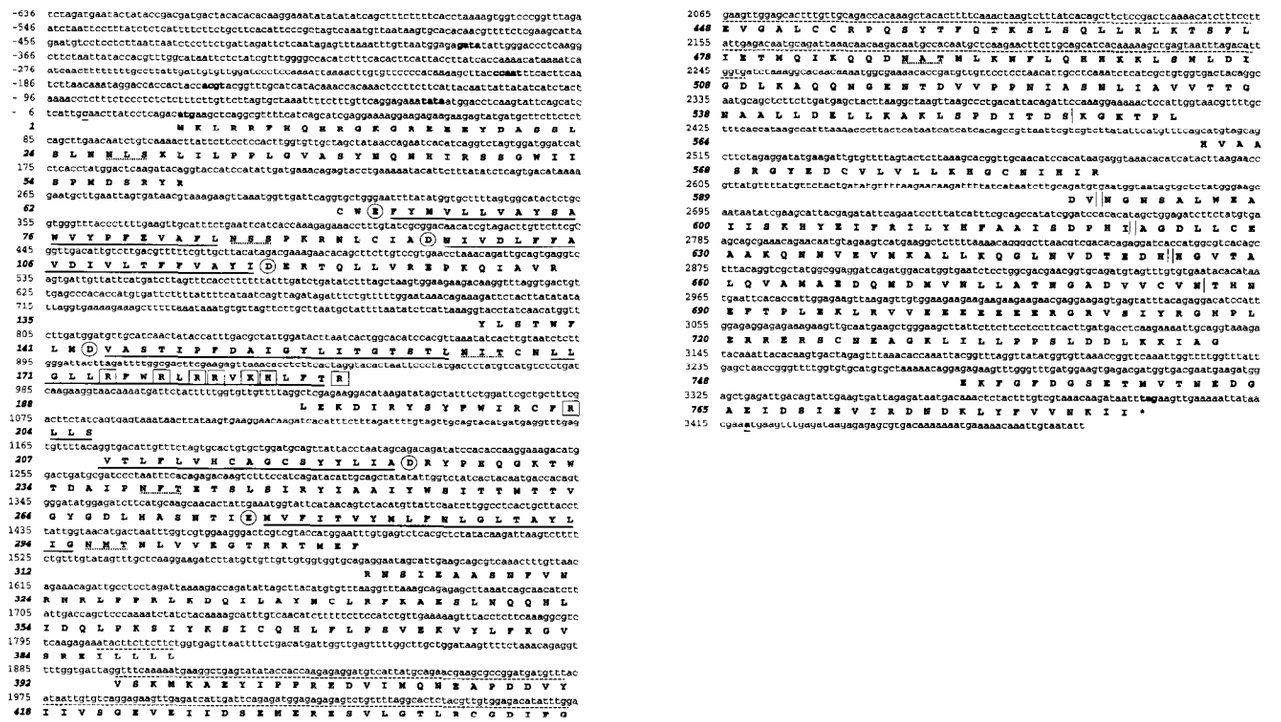

Fig. 2. Complete nucleotide sequence of the *AKT3* gene and deduced amino acid sequence from the corresponding cDNA clone. Numerical designations were made in reference to the transcriptional start site (cytosine at +1) for the nucleotide sequence, and the N-terminal methionine (*1*) for the animo acid sequence. Promoter elements in the 5′ untranslated region include a TATA box (−30 to −33), a CCAAT box (−197 to −201), the ACGT binding-sequence for basic/leucine- zipper transcription factors (−156 to −159), and the GATA light-responsive element (−384 to −387). Putative membrane spanning segments are underlined and charged residues at the border are highlighted with circles (acidic groups) or squares (basic residues). Positively charged amino acids in the fourth membrane spanning segment are also designated. Consensus sites for N-linked glycosylation are shown with a dotted underline. The nucleotide-binding domain is marked by a dashed overbar (amino acids 387 to 509). Each ankyrin repeat is enclosed by a shaded box (consensus sequence -G-TPLH-AA--GH---(V/ A)--LL--GA--(N/D)----, [33]). The poly(A) tail followed adenine 3419.

mediate the transcription of genes regulated by environmental or hormonal stimuli [22]. The second motif is the light-responsive element GATA (−384 to −387). This sequence regulates transcription of both *rbcS* (small subunit of ribulose-1,5-bisphosphate carboxylase) and *Cab* (chlorophyll a/b binding protein) and is present in the promoter region of many genes essential for photosynthesis [23].

There are nine introns in the *AKT3* genomic sequence, ranging in size from 79 to 256 bp (Table I). The GT and AG dinucleotide pairs at the intron boundaries are, as expected, invariant. Among the other nucleotides that comprise the 5′ splice junction the G at −1 and the A at +4 are most often conserved, with 7 out of 9 splice sites matching the *Arabidopsis* consensus [24]. By contrast, the 3′ splice junction exhibits more degeneracy with several nucleotides accepted at the upstream positions.

Genomic Southern blots probed with the 2.7 kb *Eco*RI fragment of the *AKT3* gene showed one major band in both *Arabidopsis* and *Nicotiana* (Fig. 3). Two minor bands were also evident in these digests, indicating the presence of additional, closely related sequences. At this stringency we did not observe cross-hybridization of the *Arabidopsis* probe with DNA from *Zea mays*, perhaps because of the tendency for noncoding regions to diverge rapidly and the evolutionary distance between dicotyledonous and monocotyledonous plants.

3.2. Structural features of the AKT3 ion channel

The predicted protein sequence of the *AKT3* gene contains 787 amino acids with a calculated molecular mass of 89,598 Daltons. There are six potential sites for N-linked glycosylation (Fig. 2), located at residues 27, 86, 164, 239, 296, and 488, and several consensus sites for protein phosphorylation by CaM kinase II (RXXS or RXXT) and protein kinase C (KXS/T or RXS/T).

Hydropathy analysis identifies 8 regions with distinct hydrophobic character, denoted as peaks with positive values for the free energy of transfer into water (Fig. 4). Five of these segments (labelled S1, S2, S3, S5, and S6) exceed the threshold value of 20 kcal/mol which correlates with stable insertion of a peptide into the lipid bilayer [25]. Each potential transmembrane segment, as illustrated in Fig. 2, has at least one boundary defined by a charged residue which may help position the peptide as part of a stop transfer sequence. The first and last peaks are significantly less hydrophobic with values of 10.3 and 15.4 kcal/mol, respectively, making it unlikely that these regions are anchored in the membrane. The final hydrophobic region, between S5 and S6 (GES value of 19.3 kcal/mol), aligns with the first half of the K^+ channel signature sequence TMTTVGYGD (amino acids 259–267). Following S3 is a segment with several positively charged animo acids organized in a fashion similar to the S4 region of other voltage-dependent

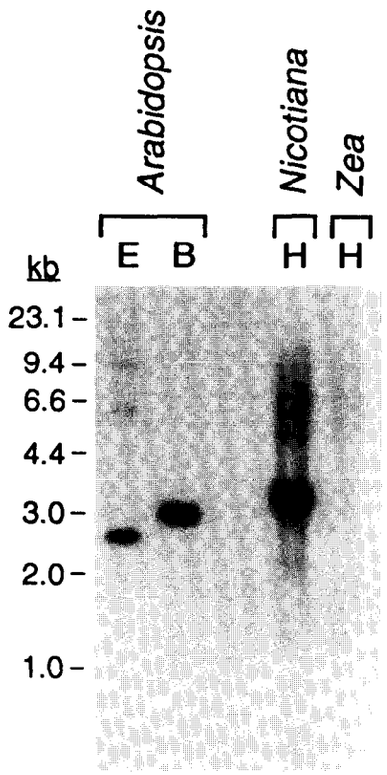

Fig. 3. Southern blot of genomic DNA from *Arabidopsis*, *Nicotiana*, and *Zea* probed with the *AKT3* genomic clone. Restriction enzymes are abbreviated as follows: E, *Eco*RI; B, *Bam*HI; and H, *Hin*dIII. Each lane was loaded with 5 μg of DNA. The 2.7 kb *Eco*RI fragment from the *AKT3* genomic clone was used to prepare a random prime-labelled probe and hybridization was done in 0.5 M $NaHPO_4$, 7% SDS, 1% BSA, 1 mM EDTA, pH 7.2 at 60°C. One major band was labelled in both *Arabidopsis* lanes at the expected size, 2.7 and 3.0 kb for the *Eco*RI and *Bam*HI digests, respectively. Two additional bands, that hybridized weakly, were also observed (6.5 and 9.4 kb, *Eco*RI; 4.0 and 6.6 kb, *Bam*HI). In *Nicotiana*, a major band at 3.3 kb cross-reacted with the *Arabidopsis* probe, and several weaker bands were found in the region between 4.4 and 7.0 kb. At this stringency, no cross-hybridization was observed with *Zea* DNA.
←

ion channels. The consensus repeat, **R/K**, X, X, observed in those proteins is represented here by **R**, F, W, **R**, L, R, **R**, V, K (residues 174 to 182). Taken together, these data suggest that AKT3 has a membrane topography similar to *Shaker*-like K^+ channels [16] with six membrane spanning segments and an ion translocating pore positioned between the last pair of helices.

The hydropathy plot also highlights two strongly hydrophilic areas at the N- and C-terminal ends of the AKT3 protein (Fig. 4). Near the C-terminus, the stretch from amino acids 690 to 731 is particularly interesting because it contains a prominent polyglutamate track, which may serve as a binding site for positively charged ions or may facilitate protein-protein interactions.

Two additional protein motifs are evident in AKT3. The first is the remnant of a cyclic nucleotide-binding domain (amino acid residues 387 to 509) which is positioned after the ion channel core. Equivalent motifs are present in cyclic nucleotide-gated channels and members of the *eag* K^+ channel family [26,27]. The parallel organization of these proteins implies that the plant *AKT3* gene shares an evolutionary ancestor with these two channel subtypes found in invertebrates and mammals. In spite of the distinct relatedness of the sequences, however, it is not clear that the cyclic nucleotide-binding domain of AKT3

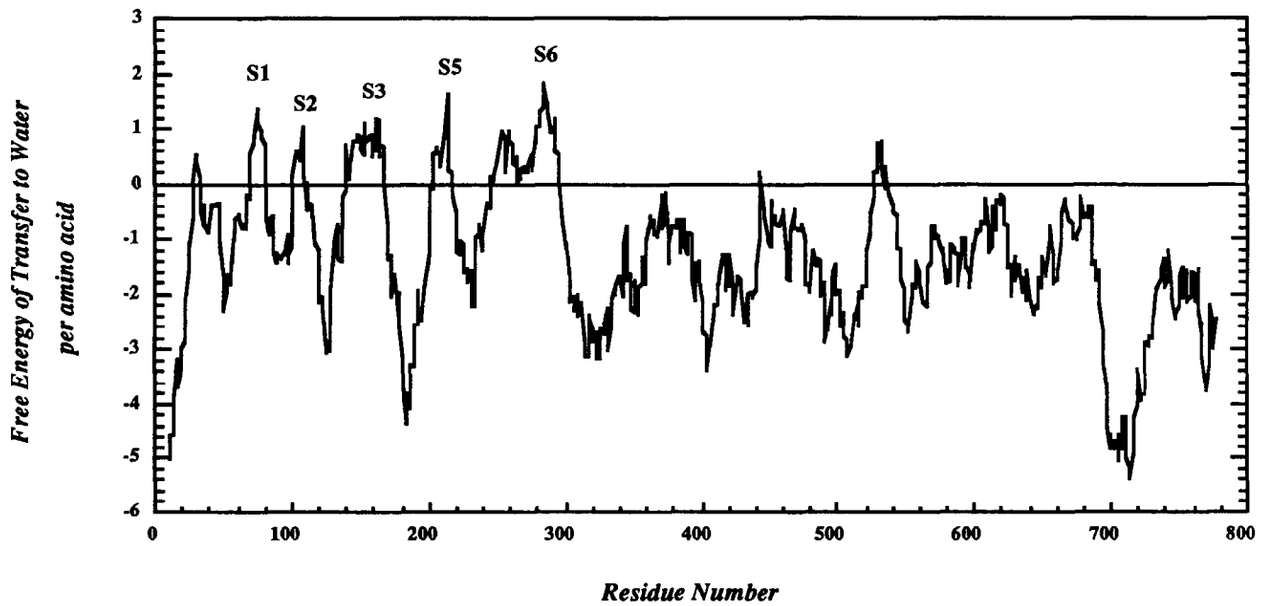

Fig. 4. Hydropathy plot of the predicted protein sequence from the *AKT3* cDNA. Average free energy of transfer to water calculated per amino acid using the algorithm of Engelman, Steitz and Goldman [25] with a window of 20 amino acids. Positive values indicate hydrophobic segments and negative numbers signify hydrophilic regions. Peaks which exceed the threshold value of 20 kcal/mol (greater than +1), required for stable insertion into the lipid bilayer, are labelled S1, S2, S3, S5, and S6 to denote potential membrane spanning segments.

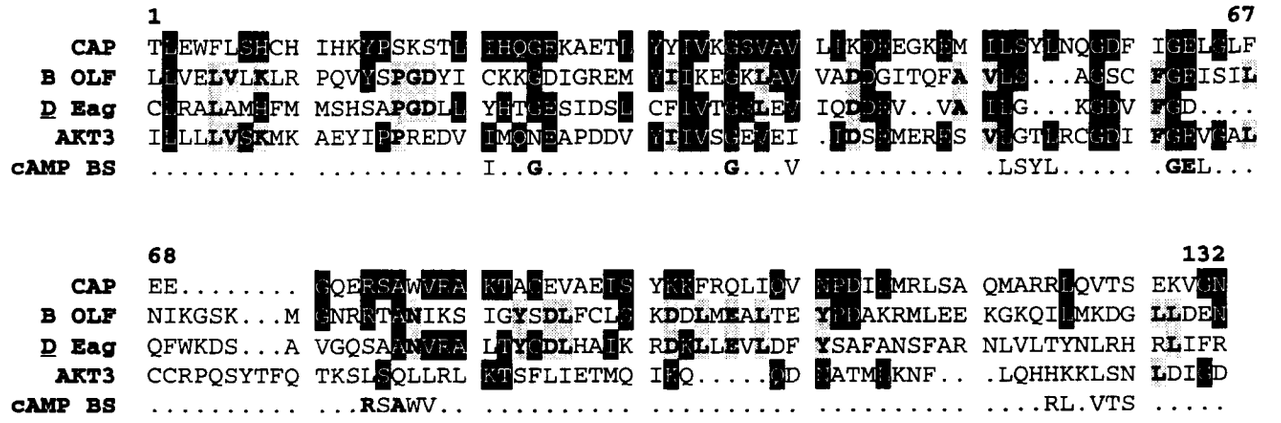

Fig. 5. Alignment of residues 387–509 from the *AKT3* protein sequence with the cyclic nucleotide-binding domains of CAP, *E. coli* catabolite gene activator protein; B OLF, bovine olfactory cyclic nucleotide-gated channel; and D Eag, *Drosophila* Eag K^+ channel. Amino acids listed in the *cAMP BS* sequence are residues highly conserved in cyclic nucleotide-binding motifs (boldface) and amino acids in contact with cAMP in the crystal structure of CAP [28]. Residues in the ion channels that are identical to the CAP sequence are boxed in black, amino acids identical to the binding site of the B OLF channel are boxed in grey.

is actually functional, since several of the amino acids which would form contact points with the phosphate of the cyclic nucleotide (defined from the crystal structure of the *E. coli* catabolite gene activator protein, CAP, reviewed in Kumar and Weber [28]) are altered in the plant gene (Fig. 5). In contrast, these same residues are well conserved in channels where cyclic nucleotides have a clear physiological effect [26,28]. It is interesting to note that many of the residues which are common to AKT3 and CAP would be in the proximity of the ribose or the adenine ring, perhaps allowing the AKT3 site to interact with other nucleotides. Single-channel recordings of excised patches from *Arabidopsis* mesophyll cells have in fact demonstrated that cytosolic ATP enhances K^+ channel activity [29]; further work will be required to determine whether the modified cyclic nucleotide domain in AKT3 can serve this alternative purpose.

Following the nucleotide-binding motif is a series of 4 ankyrin repeats (Fig. 2), encompassing residues 558 to 590, 591 to 622, 623 to 654, and 655 to 687 [30]. In this aspect AKT3 is structurally more similar to AKT1 than to KAT1 (Fig. 6, discussed below). These repeats may facilitate binding to cytoskeletal proteins allowing AKT3 to assume a specific address at the plasma membrane surface. Alternatively, the ankyrin domain may promote other types of protein-protein interaction, possibly with AKT1, other K^+ channel subunits, or cytosolic regulatory factors. It is important to bear in mind that the ankyrin repeats of AKT1 and AKT3, although similar in sequence and position, may not be functionally equivalent. Studies of erythrocyte and brain ankyrin have demonstrated that the binding affinities of these two proteins for the erythrocyte anion exchanger are not commensurate even though they share 67% sequence identity [31]. In AKT1 and AKT3, the ankyrin repeats exhibit only 36% identity.

Table I
Exon–intron splice junctions of the *AKT3* gene

	5' splice junction	3' splice junction	Intron Size
1	CAG: GTACCA	AAATG GTTGA TTCAG: G	115
2	GAG: GTCAGT	AATAT CTCAT TAAAG: G	256
3	TAG: GTACAC	TTGGT GTTGT TTTAG: G	82
4	TCA: GTGAGT	TTGAG TGTTT TACAG: G	91
5	TTT: GTGAGT	GTTGT GGTGG TGCAG: A	90
6	CTG: GTGAGT	GGTTT TGGTG ATTAG: G	79
7	TTG: GTAACG	ATATT CATGT TTCAG: C	93
8	GAG: GTAAAC	ATCAT AATCT TGCAG: A	84
9	CAG: GTAAAG	TGTGC TAAAA AACAG: G	106
	CAG: GTAAGT A	**TTTTT TTTTT TGCAG: G** P PPPP	**(P= A/G)**

Nucleotide sequence of the 5′ and 3′ boundaries of each intron are listed with the intron size. The *Arabidopsis* consensus sequence [24] is noted in bold type.

An alignment of the AKT3 protein with the other *Arabidopsis* K^+ channels shows a reasonably high degree of amino acid conservation in the N-terminal half (Fig. 6), particularly in the regions that contribute to the ion channel core and the nucleotide-binding fold. Overall the three sequences share approximately 60% identity (pair wise comparisons have values of 58.5%, AKT3 vs. AKT1; 57.5%, AKT3 vs. KAT1; and 62.8%, AKT1 vs. KAT1). These are quite similar to the values obtained when the same algorithm is used to compare *Drosophila Shaker* and *Shab* (58.3% identity) or rat Kv1.2 and Kv3.1 (57% identity) (reviewed in [16]). In contrast, more closely related proteins like rat Kv1.2 and Kv1.4 (80% identity) [16] or isoforms of the *Arabidopsis* H^+ ATPase (AHA1 and AHA2, 95% identity; AHA1 and AHA3, 89% identity) [32], have considerably fewer amino acid differences. Hence, we consider it unlikely that the three *Arabidopsis* K^+ channels, although clearly members of a gene family, are functionally equivalent. It seems plausible that the carboxyl-terminus, where amino acid differences are more conspicuous (the percent sequence identity of the region C-terminal to the nucleotide-binding domain drops to 49.6%, AKT3 vs. AKT1; 48.2%, AKT3 vs. KAT1; and 52.0%, AKT1 vs. KAT1), may be particularly important in defining the function of each ion channel.

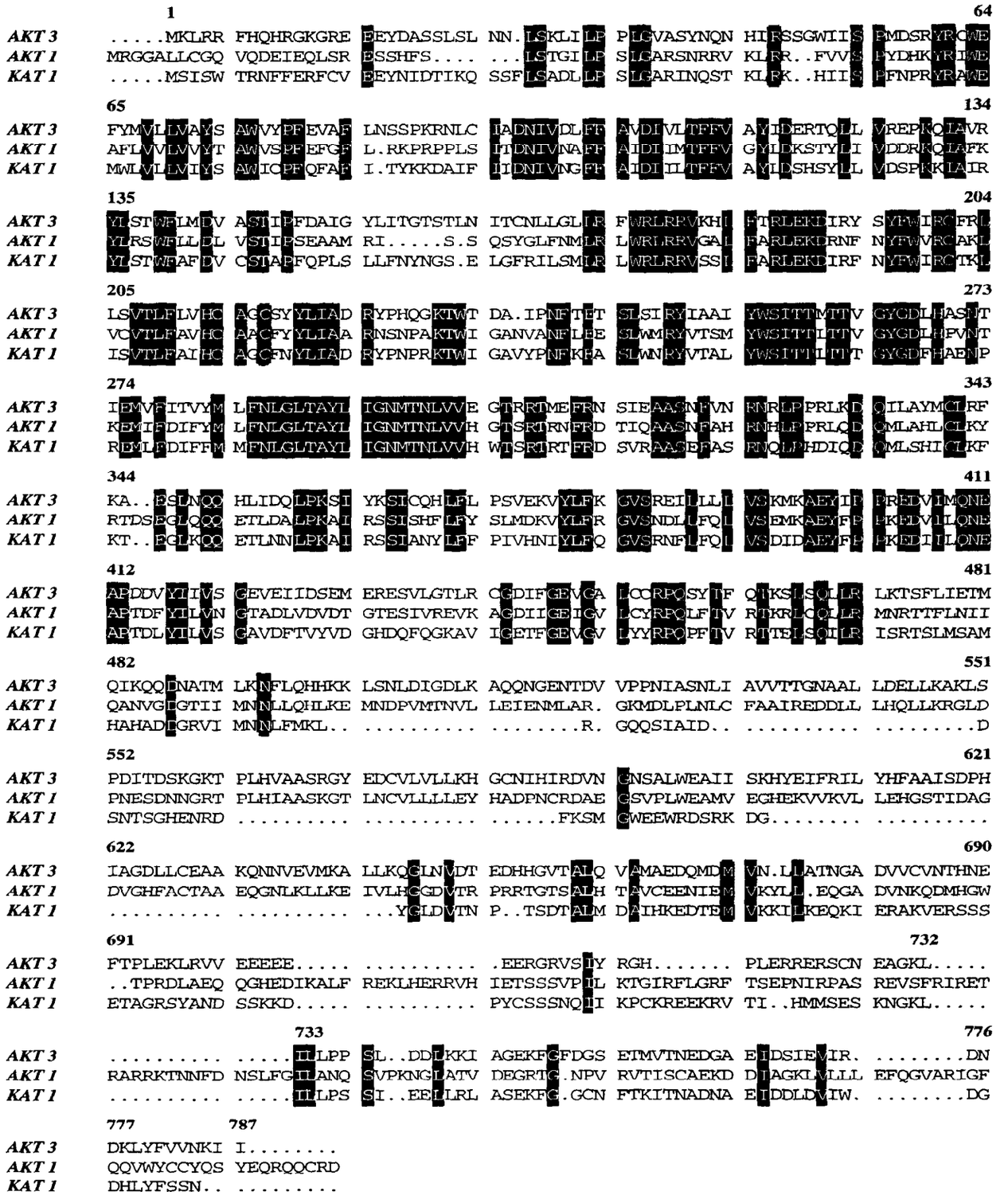

Fig. 6. Comparison of the *AKT3* amino acid sequence with the *Arabidopsis AKT1* and *KAT1* K^+ channels. Sequences were aligned with the Pileup program from the GCG software package. Numbers correspond to the *AKT3* sequence. Identical residues are boxed.

3.3. *cRNA expression in* Xenopus *oocytes*

The structural similarity between AKT3 and the other *Arabidopsis* K^+ channel proteins led us to suspect that the *AKT3* gene also encodes an inward-rectifying ion channel. To address this question, *AKT3* cRNA was expressed in *Xenopus* oocytes. Injected cells exhibited a novel inward current at test potentials

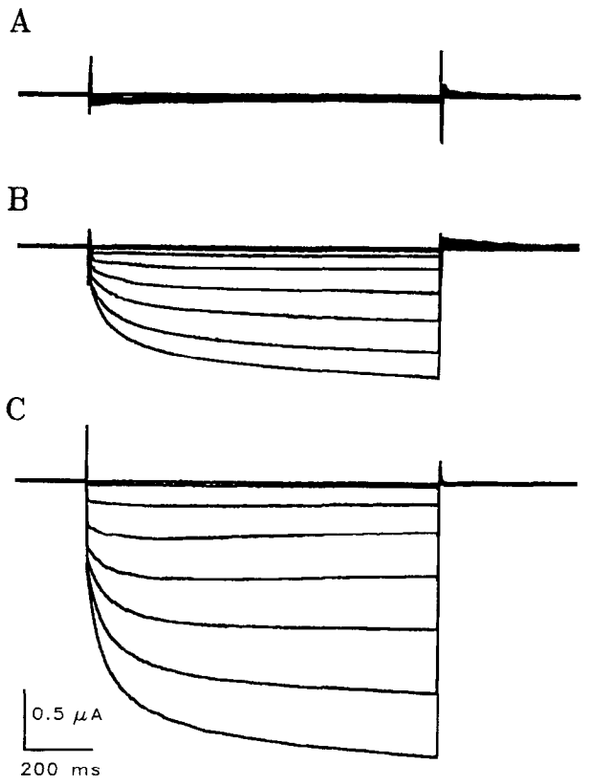

Fig. 7. Voltage-dependent currents observed in an oocyte injected with *AKT3* cRNA. Currents were recorded by two electrode voltage-clamp. The holding potential was 0 mV and test potentials ranged from 0 to −140 mV (20 mV increments). Measurements were made sequentially in three different K^+ solutions: (A) 2 mM KCl and 98 mM NaCl, (B) 20 mM KCl and 80 mM NaCl, and (C) 100 mM KCl and 0 mM NaCl. In each case, the extracellular medium also contained 0.3 mM $CaCl_2$, 1 mM $MgCl_2$, and 5 mM HEPES, pH 7.4.

more negative than −20 mV when 20 mM KCl was present in the bath (Fig. 7B). This current could be clearly distinguished from an endogenous inward-rectifier [33] by both its activation range and kinetics. No differences were observed between control and injected cells with depolarizing voltage-steps (data not shown). The AKT3 current developed with a moderately slow time-course, characteristic of K^+ inward-rectifiers from many plant species [1–4,11–15,34]. Typically, the membrane conductance increased for several milliseconds after the start of the test pulse (half-times ≅100 ms). The expressed current was sensitive to changes in external K^+ concentration: equal molar substitution of KCl by NaCl caused a marked reduction in current magnitude (Fig. 7). These results demonstrate that the AKT3 polypeptide forms a functional K^+ channel.

The voltage-activation range of *AKT3* is similar to that of the inward-rectifying K^+ channel seen in protoplasts from *Arabidopsis* suspension culture cells [34]. By contrast, channels encoded by *KAT1* activate at significantly more negative potentials, ca −100 mV [35–37], consistent with patch-clamp recordings of K^+ inward-rectifiers from other preparations. Thus, one factor that differentiates members within this gene family is the potential required for channel activation. Future studies examining the electrophysiological and pharmacological properties of *AKT3* will help distinguish this channel subtype from its sister genes, and lead to a greater understanding of its physiological role in K^+ transport.

3.4. Conclusion

AKT3 is the third member of a K^+ channel gene-family in *Arabidopsis thaliana*. It encodes a complex protein, consisting of a *Shaker*-like ion channel core associated with additional protein modules that are likely to regulate channel activity and distribution. Furthermore, the genomic sequence suggests that the physiological contribution of this channel may be controlled through transcriptional regulation, perhaps coordinating its presence with that of other proteins instrumental in photosynthesis. This observation is consistent with the fact that one of the primary jobs of plant inward-rectifying K^+ channels is to facilitate the osmotic changes required of leaf guard cells as they regulate the availability of CO_2 for carbon fixation [3].

The structure of the *Arabidopsis* K^+ inward-rectifiers also presents some interesting puzzles from an evolutionary and functional perspective. Their closest relatives are the *eag*-like K^+ channels which also have a *Shaker*-like core and a modified nucleotide-binding domain [27]. However, the *eag* gene family can encode both inward- and outward-rectifiers [27,38]. It is interesting to speculate whether other copies of the putative ancestral gene have been maintained in higher plants to encode outward-rectifying K^+ channels. If that is the case, then we might expect to find extensive sequence homologies between the inward-and outward-rectifying K^+ channels in *Arabidopsis*.

Acknowledgements: We thank Mr. Kenneth Allen for technical assistance, Dr Timothy M. Nelson (Department of Biology, Yale University) for tobacco and corn genomic DNA, and Mr. Jie Zheng and Dr. Fred Sigworth (Department of Physiology, Yale University School of Medicine) for help with oocyte expression studies. This research was supported by NSF postdoctoral fellowship DMB-9008322 to KAK and NIH research grant GM15761 to CWS.

References

[1] Tester, M. (1990) New Phytol. 114, 305–340.
[2] Schroeder, J.I., Ward, J.M. and Gassmann, W. (1994) Annu. Rev. Biophys. Biomol. Struct. 23, 441–471.
[3] Assmann, S.M. (1993) Annu. Rev. Cell Biol. 9, 345–375.
[4] Satter, R.L. (1990) in: The Pulvinus: Motor Organ for Leaf Movement (Satter, R.L., Gorton, H.L. and Vogelmann, T.C., Eds.) Current Topics in Plant Physiology: An American Society of Plant Physiologists Series Vol. 3, pp. 1–9, American Society of Plant Physiologists, Rockville, Maryland.
[5] Epstein, E., Rains, D.W. and Elzam, O.E. (1963) Proc. Natl. Acad. Sci. USA 49, 684–692.
[6] Komor, E., Cho, B., Schricker, S. and Schobert, C. (1989) Planta 177, 9–17.
[7] Kinraide, T.B., Newman, I.A. and Etherton, B. (1984) Plant Physiol. 76, 806–813.
[8] Okazaki, Y. and Tazawa, M. (1990) J. Membr. Biol. 114, 189–194.
[9] Wildon, D.C., Thain, J.F., Minchin, P.E.H., Gubb, I.R., Reilly, A.J., Skipper, Y.D., Doherty, H.M., O'Donnell, P.J. and Bowles, D.J. (1992) Nature 360, 62–65.
[10] Fairley, K., Laver, D. and Walker, N.A. (1991) J. Membr. Biol. 121, 11–22.
[11] Findlay, G.P., Tyerman, S.D., Garrill, A. and Skerrett, M. (1994) J. Membr. Biol. 139, 103–116.
[12] Schroeder, J.I. and Hagiwara, S. (1989) Nature 338, 427–430.
[13] Blatt, M.R., Thiel, G. and Trentham, D.R. (1990) Nature 346, 766–769.
[14] Blatt, M.R. (1992) J. Gen. Physiol. 99, 615–644.

[15] Fairley-Grenot, K. and Assmann, S.M. (1991) The Plant Cell 3, 1037–1044.
[16] Jan, L.Y. and Jan, Y.N. (1992) Annu. Rev. Phyisol. 54, 537–555.
[17] Anderson, J.A., Huprikar, S.S., Kochian, L.V., Lucas, W.J. and Gaber, R.F. (1992) Proc. Natl. Acad. Sci. USA 89, 3736–3740.
[18] Sentenac, H., Bonneaud, N., Minet, M., Lacroute, F., Salmon, J., Gaymard, F. and Grignon, C. (1992) Science 256, 663–665.
[19] Sambrook, J., Fritsch, E.F. and Maniatis, T. (1989) Molecular Cloning: A Laboratory Manual, 2nd edn., Cold Spring Harbor Laboratory Press, Plainview, New York.
[20] Swanson, R., Marshall, J., Smith, J.S., Williams, J.B., Boyle, M.B., Folander, K., Luneau, C.J., Antanavage, J., Oliva, C., Buhrow, S.A., Bennett, C., Stein, R.B. and Kaczmarek, L.K. (1990) Neuron 4, 929–939.
[21] Goldin, A.L. (1992) Methods Enzymol. 207, 266–279.
[22] Armstrong, G.A., Weisshaar, B. and Hahlbrock, K. (1992) The Plant Cell 4, 525–537.
[23] Gidoni, D., Brosio, P., Bond-Nutter, D., Bedbrook, J. and Dunsmuir, P. (1989) Mol. Gen. Genet. 215, 337–344.
[24] Brown, J.W.S. (1986) Nucleic Acids Res. 14, 9549–9559.
[25] Engelman, D.M., Steitz, T.A. and Goldman, A. (1986) Annu. Rev. Biophys. Biophys. Chem. 15, 321–353.
[26] Eismann, E., Bönigk, W. and Kaupp, U.B. (1993) Cell. Physiol. Biochem. 3,332–351.
[27] Warmke, J.W. and Ganetzky, B. (1994) Proc. Natl. Acad. Sci. USA 91, 3438–3442.
[28] Kumar, V.D. and Weber, I.T. (1992) Biochemistry 31, 4643–4649.
[29] Spalding, E.P. and Goldsmith, M.H.M. (1993) The Plant Cell 5, 477–484.
[30] Lux, S.E., John, K.M. and Bennet, V. (1990) Nature 344, 36–42.
[31] Davis, L.H., Otto, E. and Bennett, V. (1991) J. Biol. Chem. 266, 11163–11169.
[32] Harper, J.F., Manney, L., DeWitt, N.D., Yoo, M.H. and Sussman, M.R. (1990) J.Biol. Chem. 265, 13601–13608.
[33] Dascal, N. (1987) CRC Crit. Rev. Biochem. 22, 317–387.
[34] Colombo, R. and Cerana, R. (1991) Plant Physiol. 97, 1130–1135.
[35] Schachtman, D.P., Schroeder, J.I., Lucas, W.J., Anderson, J.A. and Gaber, R.F. (1992) Science 258, 1654–1658.
[36] Véry, A., Gaymard, F., Bosseux, C., Sentenac, H. and Thibaud, J. (1995) The Plant J. 7, 321–332.
[37] Hoshi, T. (1995) J. Gen. Physiol. 105, 309–328.
[38] Trudeau, M.C., Warmke, J.W., Ganetzky, B. and Robertson, G.A. (1995) Science 269, 92–95.